Hindawi
Geofluids
Volume 2023, Article ID 8046003, 15 pages
https://doi.org/10.1155/2023/8046003

Research Article

Damage Evolution and Constitutive Model of Marble under Dynamic Loading

Song Xie[1], **Ziyun Li**[1], **Qianghui Song**[2], **Peiyong Wang**[2], **Kaixi Xue**[3] and **Dongyan Liu**[4,5]

[1]*Chongqing University of Science and Technology, Chongqing 400000, China*
[2]*Army Logistics Academy, Chongqing Key Laboratory of Geomechanics & Geoenvironment Protection, Chongqing 400000, China*
[3]*East China University of Technology, 330000, China*
[4]*Chongqing University, Chongqing 400000, China*
[5]*Chongqing College of Architecture and Technology, Chongqing 400000, China*

Correspondence should be addressed to Song Xie; 2020206020@cqust.edu.cn and Ziyun Li; liziyun130@126.com

Received 13 December 2022; Revised 1 February 2023; Accepted 24 February 2023; Published 7 March 2023

Academic Editor: Hailing Kong

Through the application of SHPB (split Hopkinson pressure bar) test, the failure mode and dynamic stress-strain curves of marble samples were obtained. The dynamic constitutive model of marble was established with the fracture mechanical parameters (brittleness index), and the calculated curves were compared with the experimental curves. The evolution characteristic of damage variable D was analyzed. The results show that there are three main stages of marble deformation under dynamic impact load, which are linear elastic deformation stage, crack growth stage, and macroscopic failure stage. The sample shows obvious brittleness in the macroscopic failure stage. It is found that with the increase of strain rate, the degree of damage is getting worse. The stress-strain curves obtained based on the constitutive model are in good agreement with the experimental curves. The damage variable D can theoretically explain the evolution law of macroscopic failure of the sample. To some extent, there is a mechanism inside the rock to regulate the damage development of the rock, and the final failure degree of rock sample depends on $\triangle\sigma_{BC}$ and ε_b.

1. Introduction

In the process of the formation of natural rock mass and the evolution of geological structure, the dynamic disturbance is caused by seismic waves, engineering operations, and mine excavation, which leads to the rock mass spalling and mountain collapse, causing economic losses and casualties. Therefore, it is of great significance to study the mechanical properties of rocks under dynamic loads.

In the past decades, many scholars have made a lot of researches on the mechanical properties and the derivation of constitutive models under static and cyclic loads [1–6]. The deformation characteristics of rock mass under dynamic loads such as blasting and impact are often quite different from those under static loads. Therefore, it is needed to study the dynamic characteristics of rocks. Dynamic experimental research of rock is usually carried out on the SHPB system [7], failure characteristics [8, 9], energy conversion [10], etc. In terms of dynamic impact test, Kong et al. [11–13] used the dynamic constitutive model of gas bearing coal under impact load and verified the feasibility of the constitutive equation by comparing the theoretical and experimental results. Wang et al. [14] simulated the damage effect, temperature effect, and strain rate effect to the constitutive model. The constitutive model can well describe the nonlinear characteristics of frozen sandstone under impact load. Wang et al. [15] proposed a rock damage statistical constitutive model based on Weibull distribution and analyzed the influencing factors of the model parameters. The damage statistical constitutive model can accurately describe the effects of temperature and strain rate on mechanical properties of rocks. Deng and Gu [16] incorporated the entropy distribution information

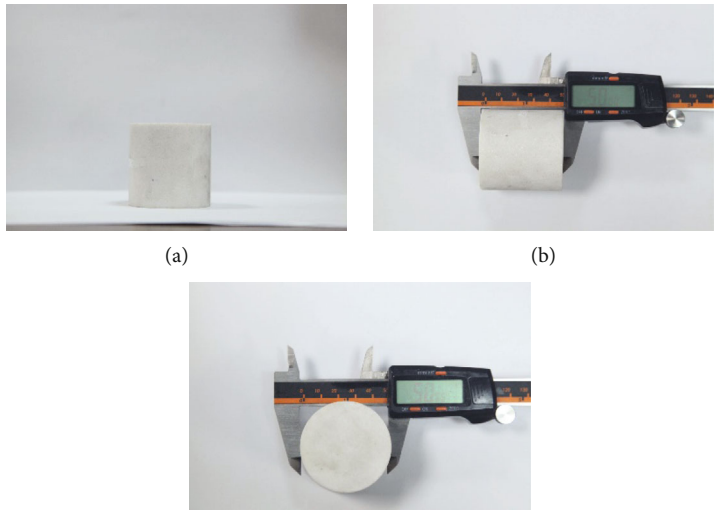

(a) (b) (c)

Figure 1: The measurement of sample size. (a) Sample, (b) height, (c) diameter.

into a damage variable and derived a new constitutive model. Zhai et al. [17] applied the energy principle to the constitutive model, which is closer to the experimental results than previous damage constitutive models based on energy. Zhao et al. [18] combined the continuous damage theory and statistical strength theory into the development of the simplified constitutive formula of the stress and developed a damage-based overstress model.

All these studies have greatly promoted the development of rock dynamics. However, few scholars have used the SHPB system to study the postpeak failure behavior and the evolution law of damage variables of rocks at high strain rates. In this paper, the dynamic constitutive model of marble under different strain rates was proposed in combination with fracture mechanics theories. And the damage evolution of rock samples under dynamic impact loads was analyzed. The postpeak dynamic fracture mechanism of rock and the damage and failure mechanism of rock under dynamic load were revealed.

2. Experimental Design

2.1. Sample Preparation. The samples were taken from Leiyang, Hunan Province, and the samples are processed in strict accordance with the specifications of the International Society for Rock Mechanics [19]. The diameter and height of the sample are both 50 mm, and the nonparallelism of the upper and lower end faces is guaranteed to be no more than 0.02 mm. Sample length and diameter measurements are showed in Figure 1. Prior to the sample preparation, the basic mechanical parameters of the rock were characterized [20, 21]. The specific parameters of the marble are as follows: the density is 0.7 g/cm^3, a uniaxial compressive strength (UCS) of 114.7 MPa, and the P-wave velocity is 2631 m/s.

2.2. Experimental Equipment. The dynamic impact experiment was carried out on the split Hopkinson pressure bar in Central South University, China. The half-period sine wave generated by the spindle bullet used in the device avoids the waveform distortion generated by the traditional cylindrical punch, thus realizing the constant strain rate loading. SHPB test system solves the problem of stress and strain measurement [22]. It is widely used to study the dynamic mechanical properties of materials [23], such as the dynamic tensile experiments [24, 25] and other dynamic impact experiments [26]. The whole system consists of spindle-shaped bullet, incident bar (2 m in length), transmission bar (1.5 m in length), absorption bar (0.8 m in length), DL850E oscilloscope, CS1D dynamic strain gauge, and a high-speed camera. The pressure bar is made of 40Cr alloy, the density is 7837 kg/m^3, the P-wave velocity is 5470 m/s, and the elastic modulus is 240 GPa. The SHPB system is shown in Figure 2.

A high-speed camera was used to record the failure patterns and crack growth of rock samples during the experiment. The shooting frequency was 3000 times/s. And the whole process from crack to complete failure can be clearly observed.

2.3. Experimental Procedure. The main purpose of this experiment is to study the failure characteristics and mechanical properties of rock mass with different strain rates. Therefore, pretests were carried out before the formal experiment to ensure the rock sample failure under the minimum impact pressure. After several tests, five levels of impact pressures were finally determined. From low to high, they are 0.5 MPa, 0.525 MPa, 0.55 MPa, 0.575 MPa, 0.6 MPa, and 0.625 MPa, respectively. In order to systematically investigate the effect of strain rate on rock properties, five different air pressures were selected. Each test was repeated three times under the same air pressure to ensure a similar impact loading rate.

2.4. Experimental Procedure. Before the experiment, the strain gauges were pasted on the incident bar and the

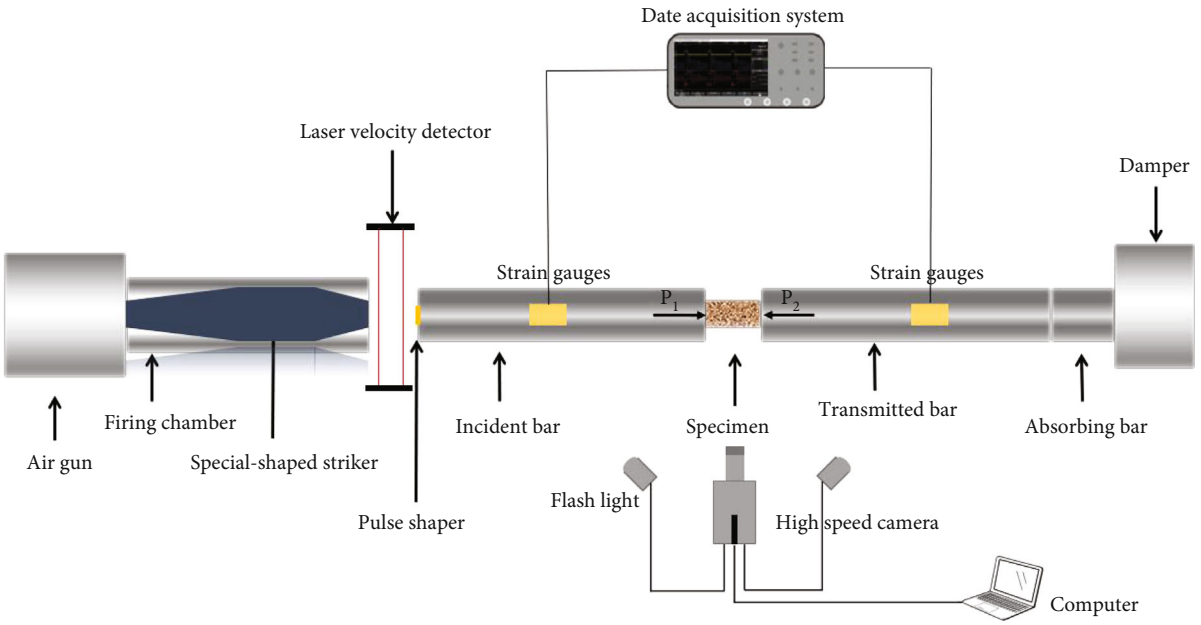

(a)

(b)

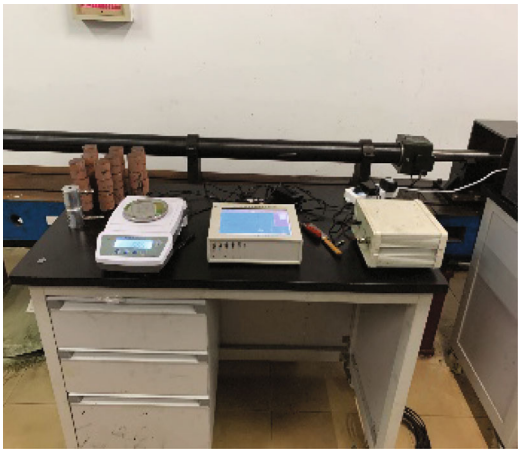

(c)

(d)

Figure 2: SHPB system and test equipment. (a) SHPB system, (b) data acquisition system, (c) electronic scale and wave velocity meter, (d) high-speed camera.

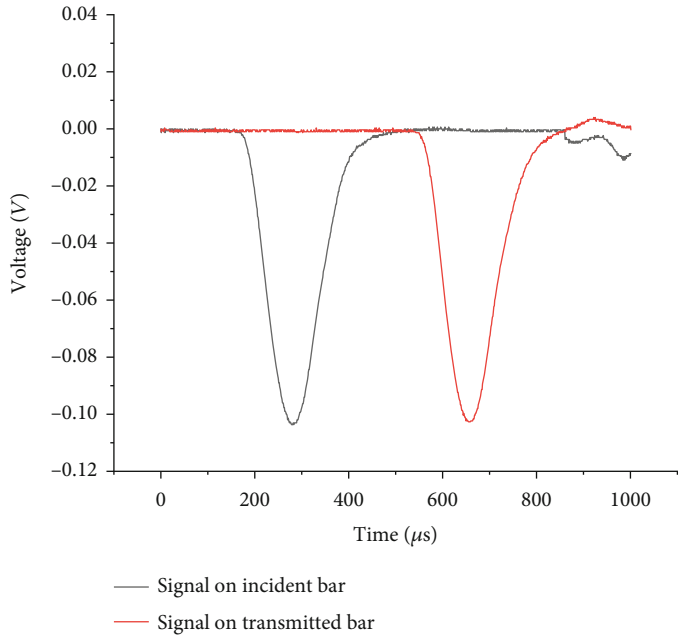

Figure 3: Electrical signals of preimpact.

transmission bar, respectively. When the bullet was emitted from the air chamber and hit the incident bar, the strain gauge on the incident bar detected the incident stress wave, and the reflected stress wave and the transmitted stress wave would be detected by the strain gauges on the incident bar and the transmission bar, respectively. According to theory of one dimension stress wave

$$\sigma(t) = \frac{[\sigma_I(t) - \sigma_R(t) + \sigma_T(t)]A_e}{(2A_s)},$$
$$\varepsilon(t) = \frac{1}{\rho_e C_e L_s}\int_0^t [\sigma_I(t) + \sigma_R(t) - \sigma_T(t)]dt, \quad (1)$$
$$\dot{\varepsilon}(t) = \frac{1}{\rho_e C_e L_s}[\sigma_I(t) + \sigma_R(t) - \sigma_T(t)].$$

$\sigma(t)$, $\sigma_I(t)$, $\sigma_R(t)$, and $\sigma_T(t)$ are the dynamic stress, incident stress, reflected stress, and transmitted stress, respectively. $\varepsilon(t)$ and $\dot{\varepsilon}$ are strain and strain rate, and A_S and L_S are the cross-sectional areas and length of sample. A_e, ρ_e, C_e are the cross-sectional areas, density and P-wave of bar.

Preimpact experiment shall be carried out before the formal experiment to ensure that the SHPB system is in good condition. The preimpact electrical signal time diagram is shown in Figure 3.

The voltage-time and stress wave-time curves are shown in Figures 4(a) and 4(b). The sum of the incident stress wave and the reflected stress wave is almost equal to the transmitted stress wave, indicating that the two ends of the sample have reached the stress equilibrium state, which has effectively reduced the wave dispersion and inertial effect.

3. Experimental Results

3.1. Mechanical Behavior. As a kind of rock formed by metamorphism of carbonate rocks in sedimentary rocks, marble has higher hardness than sand and sandstone, and its mechanical properties under dynamic impact load also show different characteristics. The dynamic stress-strain curve of marble specimens can be divided into three stages according to the failure process, which are the linear elastic stage (no cracks in the rock sample), crack propagation stage (crack generation and propagation), and macrofracture stage (macrofracture surface generation), respectively. Figure 5 shows the typical dynamic stress-strain curve of marble, which can be divided into three stages [27]. In the initial stage (OA stage), different from the initial stage under static loading, the dynamic stress-strain curve does not show obvious depression. This is because under the impact load, the microcracks in the rock have no time to be connected, so there is no obvious compaction stage. The stress shows a linear growth trend with the increase of strain. In the crack initiation and growth stage (AB stage), before reaching the peak strength, the growth rate of stress with strain slows down, and the modulus of deformation decreases. At this stage, the internal microcracks of rock samples begin to expand. Point B is the crack nucleation point, and the strain corresponding to point B is usually 2/3 of the peak strength, because the compressive strain often suddenly drops to negative values when it slowly goes down to the point about two thirds of the peak value after the peak [28]. The stage from peak strength to point B is the stage of crack nucleation, that is, under the action of stress or environmental factors or the combination of the two, the process of crack propagation in an intact specimen. BC stage is macrofailure stage; when the macrofracture surface forms, the stress in this stage drops

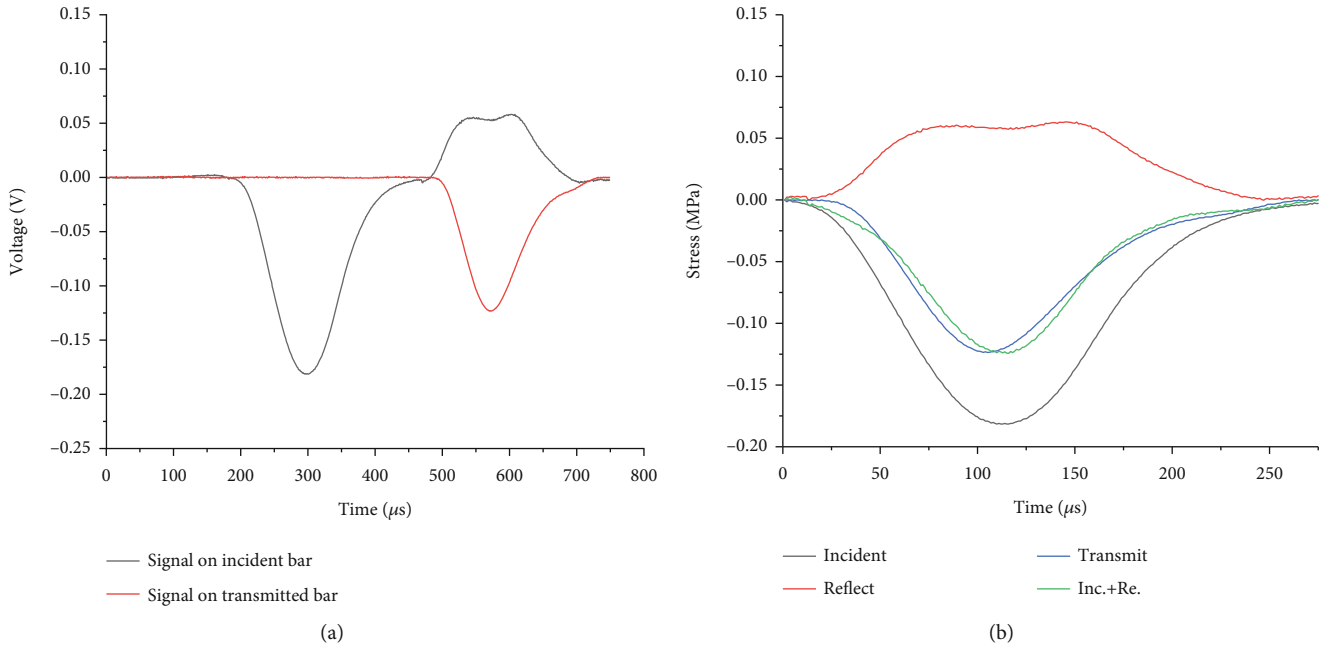

Figure 4: The voltage-time and stress wave-time curves. (a) The voltage time, (b) stress wave time.

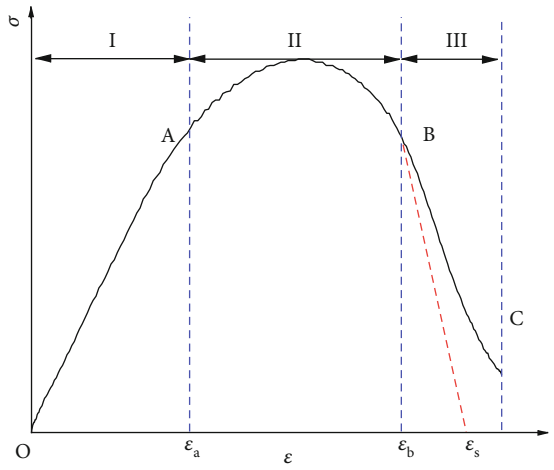

Figure 5: Damage evolution of marble.

rapidly, showing obvious brittle characteristics. ε_a is the strain corresponding to the beginning of stage AB, ε_b is the strain corresponding to the end of stage AB, and ε_s is the strain corresponding to the end point of brittle fracture.

3.2. Energy Evolution Characteristics. According to the experimental results, stress-strain curves of marbles under impact at different strain rates are drawn in Figure 6. The stress-strain curves are similar at different strain rates. The peak strength increases with the increase of strain rate, showing an obvious strain rate effect.

The relationship between peak stress and peak strain and strain rate can be obtained from the experimental data. Plot the relationship between peak stress and peak strain (Figure 7). It can be found that with the increase of strain rate, the peak strain and peak stress increase gradually. The relationship between peak strain and peak stress and strain rate can be expressed by linear relation:

$$\begin{aligned} \varepsilon_{\max} &= 0.00007\dot{\varepsilon} + 0.0003, \\ \sigma_{\max} &= 2.9\dot{\varepsilon} + 13.81. \end{aligned} \tag{2}$$

3.3. Damage Characteristics of Specimens under Cyclic Loading. During the test, the cracking process of rock samples was recorded by using a high-speed camera. Failure photos of samples with the same time interval are selected from the beginning of crack generation. The typical failure process of samples under impact load is shown in Figure 8. The failure mode of marble samples in this test is tensile failure. It can be seen from Figure 8 that in the initial loading stage, cracks appear on the surface of the sample. With the increase of strain rate, the crack length gradually increases, the damage degree of the rock sample gradually increases, and the powdered fragments increase. The cracks of rock sample expand rapidly, forming macroscopic fracture surface. At low strain rate, the number of cracks in rock samples impacted is less. With the increase of strain rate, the crack growth rate of rock sample becomes faster, the number of cracks increases gradually, and the crack position turns from the edge to the middle. The corresponding strain rates of ABCDE are 34.72 s^{-1}, 45.22 s^{-1}, 50.34 s^{-1}, 59.97 s^{-1}, and 67.32 s^{-1}, respectively.

4. Constitutive Model

4.1. Derivation of Constitutive Model Based on Damage Variable. The dynamic damage evolution process is similar

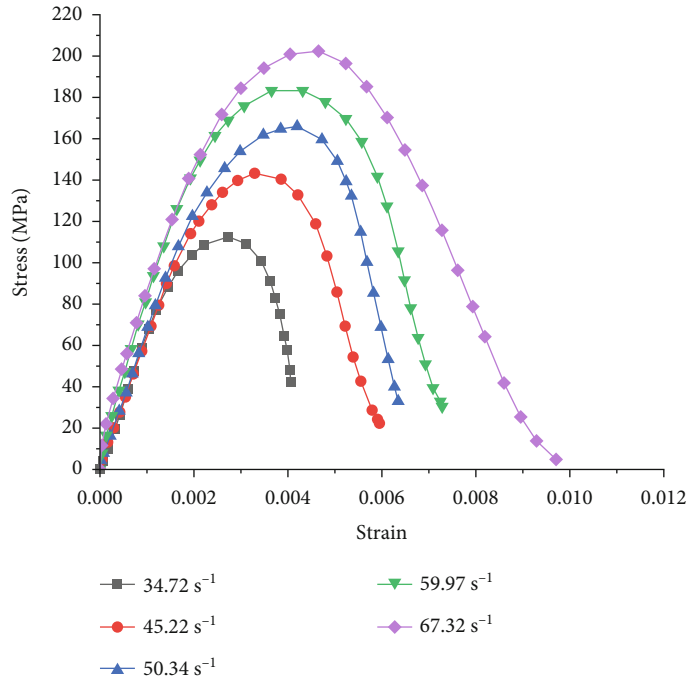

Figure 6: Curves of dynamic stress-strain at different strain rates.

to that under static loading. The damage evolution process of marble mainly includes I (linear elastic stage), II (crack initiation and development stage), and III (macroscopic fracture surface formation stage). The damage variable in OB stage is defined as [29]

$$D = \left(\frac{\varepsilon}{\varepsilon_s}\right)^{\lambda}, \tag{3}$$

where ε is the strain; ε_s is the strain corresponding to the end point of brittle fracture. λ is the brittleness index.

According to the research results of elastic mechanics and related references, the constitutive relation of rock considering damage characteristics can be expressed as [30]

$$\sigma_1 = E_D\left(1 - \left(\frac{\varepsilon}{\varepsilon_s}\right)^{\lambda}\right)\varepsilon. \tag{4}$$

The dynamic elastic modulus E_D is the slope corresponding to the linear phase on the dynamic stress-strain curve.

The stress-strain equation of BC stage is defined as

$$\sigma_2 = \mathrm{a}e^{\varepsilon} + b, \tag{5}$$

where a and b are the parameters obtained by solving the equations. The stress-strain curves drawn according to equations (4) and (8) are smoothly connected at point B; that is, the two curves are continuous and have the same slope at point B. According to equations (4) and (8), the slope corresponding to point B is k_a and k_b, respectively.

$$\begin{aligned} k_a &= E_D\left[1 - \left(\frac{\varepsilon_b}{\varepsilon}\right)^{\lambda}(\lambda + 1)\right], \\ k_b &= \mathrm{a}e^{\varepsilon_b}, \\ k_a &= k_b. \end{aligned} \tag{6}$$

ε_b is the strain corresponding to point B, which represents the strain at the completion of macroscopic crack nucleation.

The solving coefficients a and b can be obtained by combining the above equations ((7)–(10)).

$$\begin{aligned} a &= \frac{E_D\left(1 - (\varepsilon_b/\varepsilon_s)^{\lambda}\right)(\lambda + 1)}{\varepsilon_b}, \\ b &= E_D\left(1 - \left(\frac{\varepsilon_b}{\varepsilon_s}\right)^{\lambda}\right)\varepsilon_b - \frac{E_{\mathrm{D}}\left(1 - (\varepsilon_b/\varepsilon_s)^{\lambda}\right)(\lambda + 1)}{\varepsilon_b}e^{\varepsilon_b}. \end{aligned} \tag{7}$$

To simplify the calculation, the marble sample lost its bearing capacity under dynamic impact load, and the curve drops rapidly, so the stress dropping is introduced:

$$\Delta\sigma_{\mathrm{BC}} = E_D\left(1 - \left(\frac{\varepsilon_b}{\varepsilon_s}\right)^{\lambda}\right)\varepsilon_b. \tag{8}$$

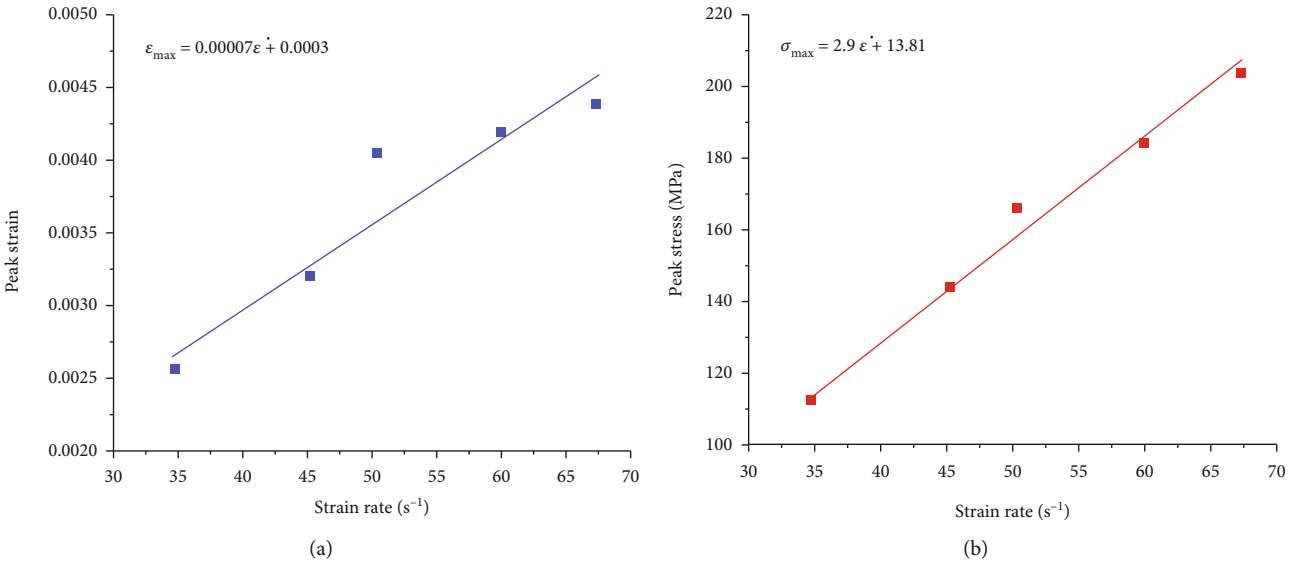

Figure 7: The relationship between peak strain and peak stress with strain rate. (a) Peak strain, (b) peak stress.

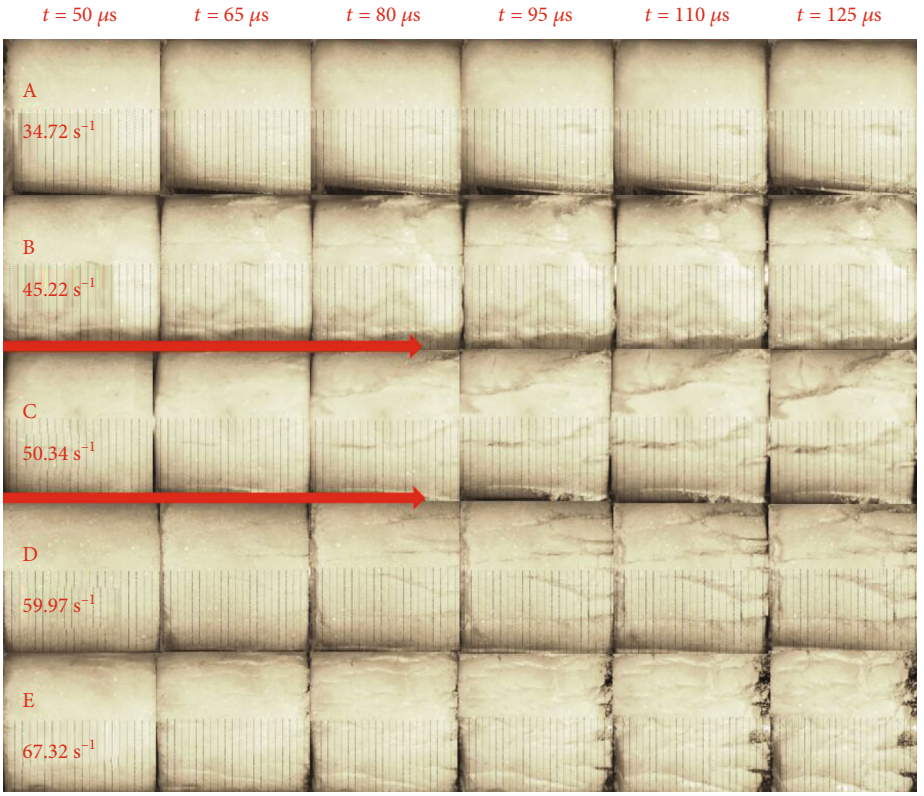

Figure 8: High-speed photography of crack process (impact from left to right).

a, b, and $\Delta\sigma_{BC}$ are substituted into equation (8) to obtain the stress-strain equation of BC stage:

$$\sigma = \frac{k}{\varepsilon_b} e^{\varepsilon} + \Delta\sigma_{BC} - \frac{k e^{\varepsilon_b}}{\varepsilon_b} = \frac{k}{\varepsilon_b}\left(e^{\varepsilon} - e^{\varepsilon_b}\right) + \Delta\sigma_{BC}. \quad (9)$$

σ can also be expressed as

$$\sigma = \frac{k}{\varepsilon_b}\left(e^{\varepsilon} - e^{\varepsilon_b}\right) + \Delta\sigma_{BC} = E_D(1 - D)\varepsilon. \quad (10)$$

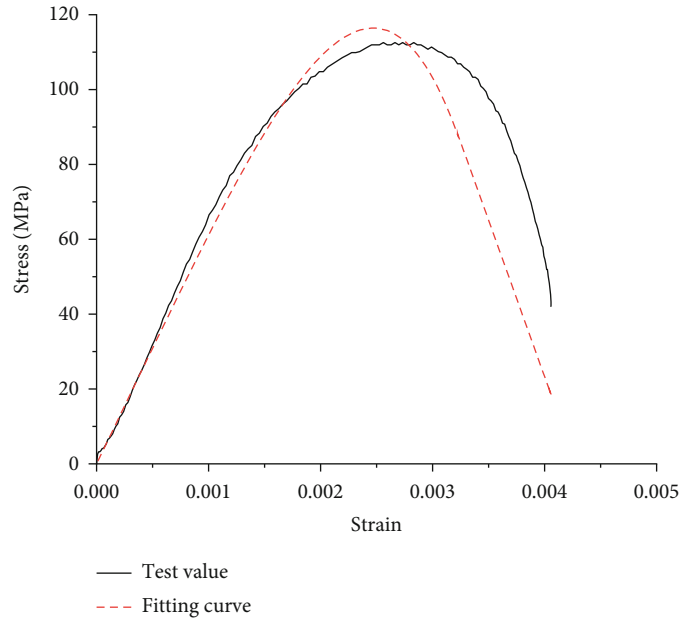

(a)

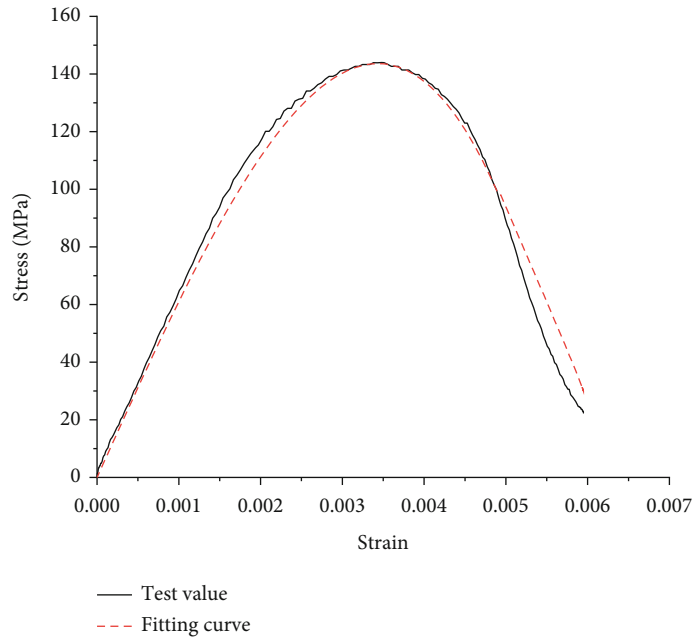

(b)

Figure 9: Continued.

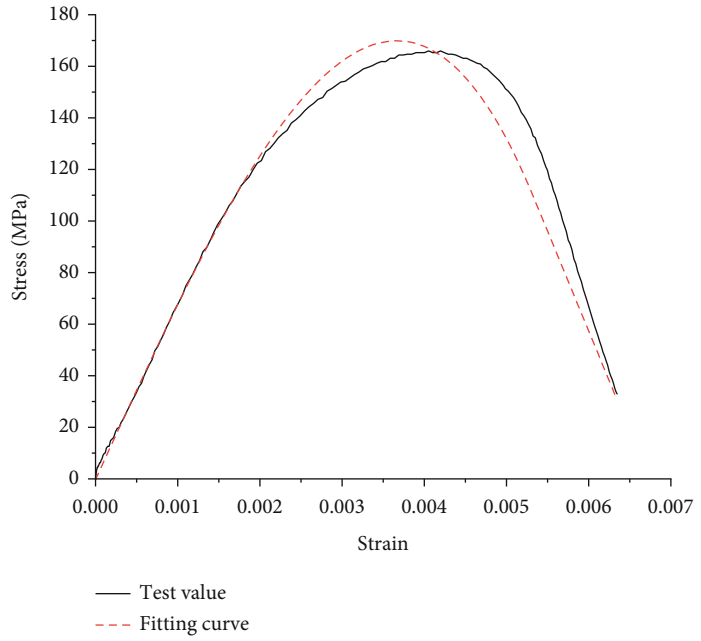

(c)

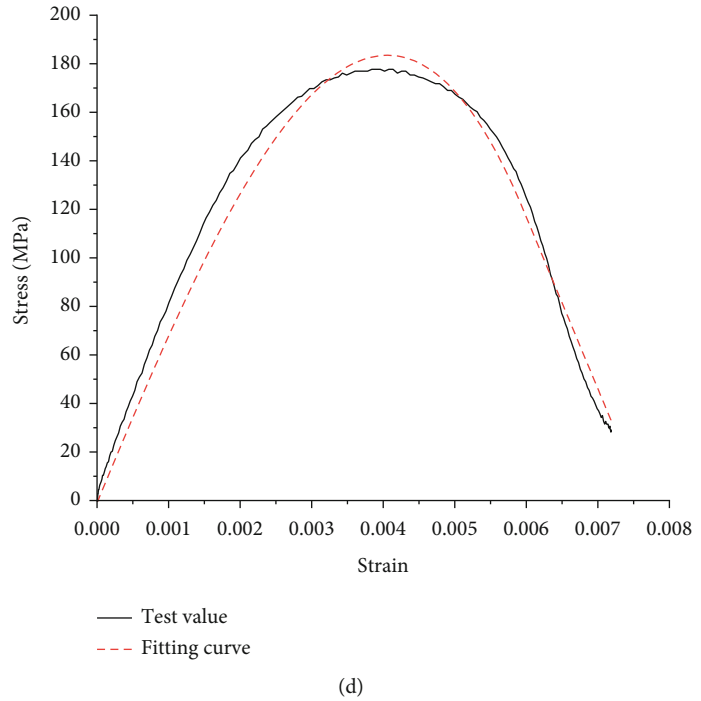

(d)

Figure 9: Continued.

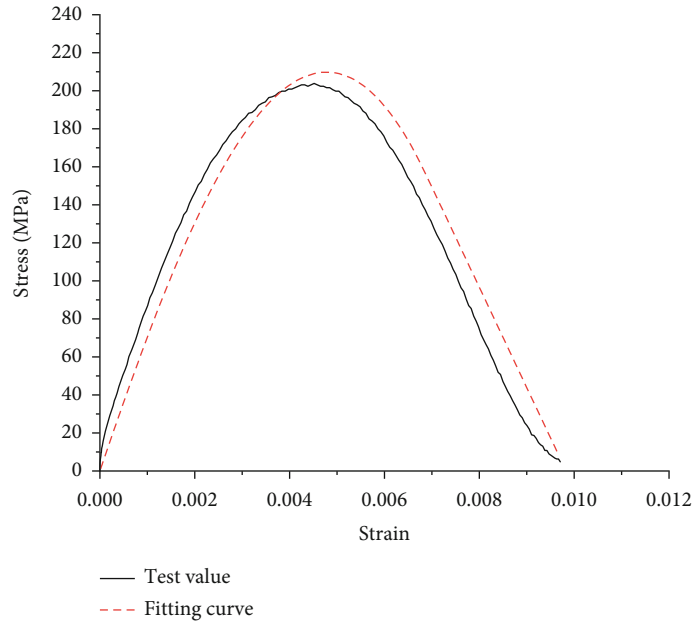

(e)

Figure 9: Comparison between stress-strain measured and fitting curves: (a) 34.72 s^{-1}, (b) 45.22 s^{-1}, (c) 50.34 s^{-1}, (d) 59.97 s^{-1}, (e) 67.32 s^{-1}.

Table 1: Correlation between model parameters and test data.

Sample number	$\dot{\varepsilon}$	E_D	ε_b	ε_s	λ
A	34.7	61.92	0.0032	0.0039	3.2
B	45.2	62.73	0.0049	0.0059	2
C	50.3	69.56	0.0053	0.0063	1.9
D	60.0	71.89	0.006	0.0073	1.7
E	67.3	73.18	0.0069	0.0088	1.5

The damage variable of the BC Stage is obtained:

$$D = 1 - \left(\frac{(k/\varepsilon_b)(e^{\varepsilon} - e^{\varepsilon_b}) + \Delta\sigma_{\mathrm{BC}}}{E_D \varepsilon} \right). \tag{11}$$

Then, the whole process damage variable of marble under dynamic impact load can be expressed as

$$\begin{aligned} D &= \left(\frac{\varepsilon}{\varepsilon_s} \right)^{\lambda}, \ \varepsilon < \varepsilon_b, \\ D &= 1 - \left(\frac{(k/\varepsilon_b)(e^{\varepsilon} - e^{\varepsilon_b}) + \Delta\sigma_{\mathrm{BC}}}{E_D \varepsilon} \right), \quad \varepsilon > \varepsilon_b. \end{aligned} \tag{12}$$

The whole process stress-strain equation of marble under dynamic impact load can be expressed as

$$\begin{aligned} \sigma &= E_D \left(1 - \left(\frac{\varepsilon}{\varepsilon_s} \right)^{\lambda} \right) \varepsilon, \qquad \varepsilon < \varepsilon_b, \\ \sigma &= \frac{k}{\varepsilon_b} (e^{\varepsilon} - e^{\varepsilon_b}) + \Delta\sigma_{\mathrm{BC}}, \quad \varepsilon > \varepsilon_b. \end{aligned} \tag{13}$$

In this section, the relevant parameters of dynamic damage constitutive model of marble were obtained from the experimental data, which include dynamic elastic modulus E_D, brittleness index λ, strain ε_b corresponding to crack nucleation point, and extreme strain ε_s. However, it is necessary to ensure that the parameters E_D, ε_b, and ε_s are positively correlated with the strain rate, while the brittleness index λ is negatively correlated with the strain rate [31]. The obtained fitting curves are shown in Figure 9, and the relevant parameters are shown in Table 1. The obtained fitting curves were basically consistent with the experiment curves and meet the requirements of the fitting curves.

Both Figure 9 and Table 1 well verify the adaptability of the model at different strain rates, which can accurately indicate the dynamic mechanical properties of marble.

4.2. The Evolution of D. In Section 4.1, the dynamic damage constitutive model of marble was derived, and the dynamic stress-strain curves and damage parameter D of marble were obtained. As a damage variable, D can characterize the damage conditions of marble at different stages. In this section, the variation of D with strain during dynamic impact of different rock samples at different strain rates was discussed.

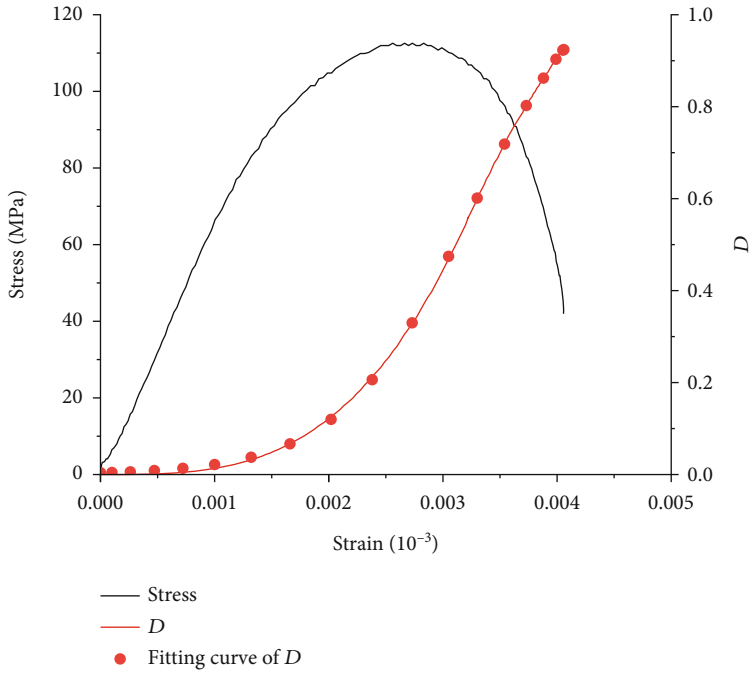

(a)

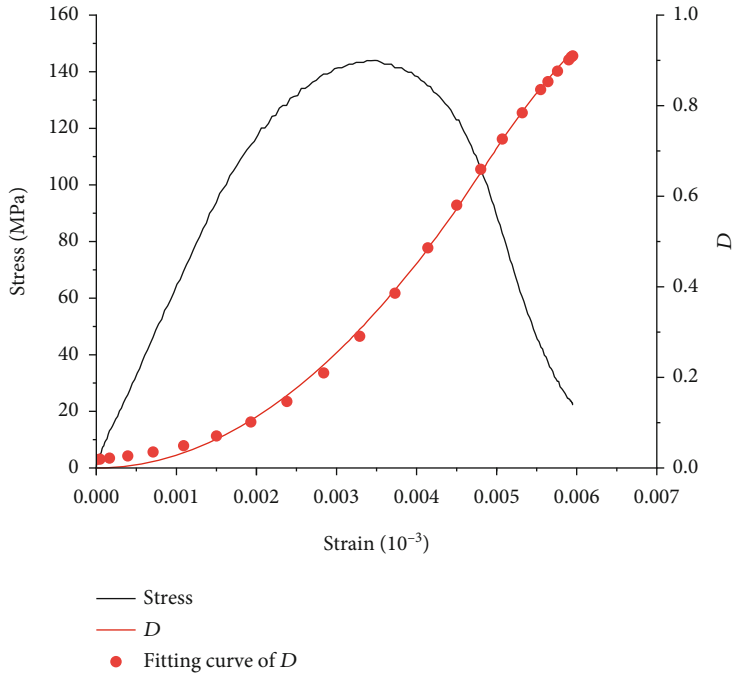

(b)

Figure 10: Continued.

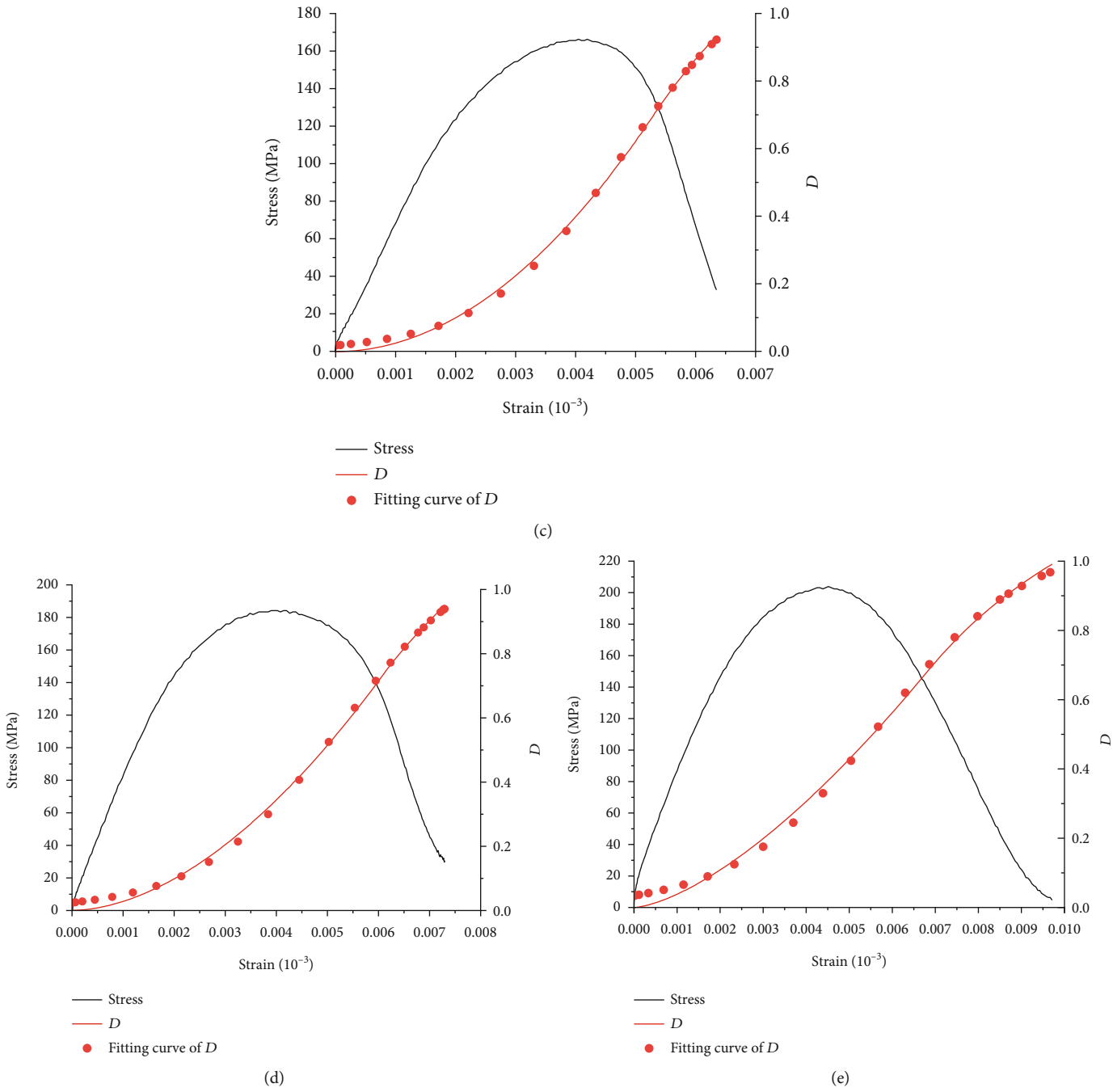

Figure 10: Stress-strain curves and D-strain curves: (a) 34.72 s^{-1}, (b) 45.22 s^{-1}, (c) 50.34 s^{-1}, (d) 59.97 s^{-1}, (e) 67.32 s^{-1}.

The variation trend of D with strain at different strain rates was basically the same. As can be seen from Figure 10, in the dynamic impact process, the variation trend of D with strain presents an "S" shape, which develops steadily at the initial stage, then increases rapidly, and finally becomes stable. By comparing the stress-strain curve with the D-strain curve, it can be seen that the variation trend of damage D well reflects the three stages of rock deformation.

By fitting the test data, the variation law of D of marble under different strain rates at characteristic points, as shown in Figure 10, and the expressions of D and ε are showed in Table 2.

Table 2: Fitting equations of samples under different strain rates.

Sample number	Equation	R^2
A	$D = 1.149/1 + e^{-1.755\varepsilon 10^3 + 2.016}$	0.99
B	$D = 1.147/1 + e^{-0.921\varepsilon 10^3 + 4.11}$	0.99
C	$D = 1.16/1 + e^{-0.865\varepsilon 10^3 + 4.144}$	0.99
D	$D = 1.139/1 + e^{-729\varepsilon 10^3 + 3.843}$	0.99
E	$D = 1.062/1 + e^{-0.593\varepsilon 10^3 + 4}$	0.99

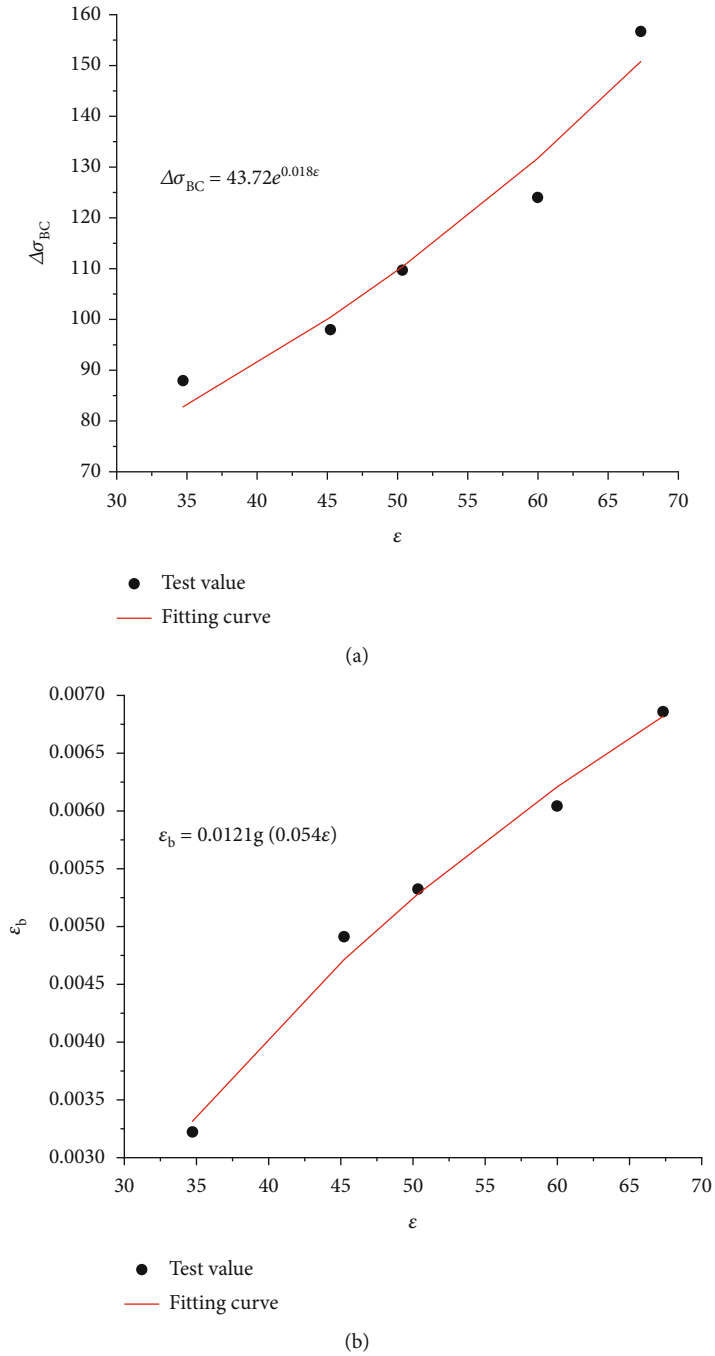

Figure 11: The relationship between $\triangle\sigma_{BC}$, ε_b, and strain rate. (a) $\triangle\sigma_{BC}$, (b) ε_b.

There are many self-promotion and self-inhibition mechanisms for rock under impact loading, and each mechanism has a certain effect on rock stably (compaction and crack generation). Taking D as an example, in the initial stage of loading, D slowly increases with the increase of strain, which corresponds to the linear elastic stage (OA stage). At this time, the rock sample is compacted, and there is almost no damage to the rock sample. This is because there is a mechanism inside the rock sample that prevents the rock sample from being completely compacted, and D grows slowly. After the rock sample is completely compacted, the cohesion between the rock sample structures needs to be overcome when the rock sample enters the damage state from the intact state. Once the cohesion of the rock sample fails due to external conditions, the damage stage starts, and microcracks (BC stage) begin to appear inside the rock sample. At this time, some mechanism inside the rock sample will promote the damage growth, which is shown by the crack expansion, and the growth rate of D value is accelerated. When cracks nucleate, the growth of damage variable D slows down. it shows the self-inhibition effect inside the rock sample. At this time, the macrocracks

begin to expand (BC stage), forming a macrofailure surface. At point C, the damage variable D reaches the maximum, and the rock sample loses strength. It indicates that there are some self-promotion and self-inhibition in the rock sample [32, 33].

5. Discussion

According to Meng et al. [34, 35], the magnitude of postpeak stress dropping is the external manifestation of the degree of brittle failure of rock. It can be seen from the Figure 11 that with the increase of strain rate, σ_{BC} and ε_b show linear different trend. In combination with the failure process of samples (Figure 8), the law obtained in this paper is the same as that.

In Section 4.1, the constitutive model of the marble sample was derived, and according to the experimental curves and related theories, the damage and failure parameters $\triangle\sigma_{\mathrm{BC}}$ and strain ε_b of the crack nucleation point of the marble are solved. $\triangle\sigma_{\mathrm{BC}}$ is the stress dropping upon completion of crack nucleation, and ε_b represents the deformation characteristics of marble under dynamic impact load. $\triangle\sigma_{\mathrm{BC}}$ increases exponentially with the increase of strain rate, and ε_b increases logarithmically with the increase of strain rate. The variation trend of brittleness parameters with strain rate is shown in Figure 11. Therefore, the strain rate may have a stronger effect on $\triangle\sigma_{\mathrm{BC}}$ than on ε_b. Subsequently, in order to understand the effect of strain rate on brittle fracture of rock, multiple sets of dynamic impact tests under different strain rates will be conducted to explore the influence of strain rates on brittleness parameters.

6. Conclusions

(1) The deformation stage of marble under dynamic loading can be divided into three stages: linear elastic stage, the crack initiation and growth stage, and macrofailure surface stage. The peak strain and stress of marble increase with the increase of strain rate, and the higher the strain rate is, the faster the crack grows

(2) Based on the theory of fracture mechanics, the constitutive model considering the brittleness index of marble is derived. The constitutive model can well describe the dynamic mechanical properties of marble under dynamic impact

(3) The development trends of damage variables in the three stages of marble deformation are different. There is some mechanism in the rock sample to regulate the damage development of the rock

(4) The stress dropping $\triangle\sigma_{\mathrm{BC}}$ and ε_b increase with the increase of strain rate. However, with the increase of strain rate, the increase degree of the two is different. The final failure degree of rock sample depends on them

Data Availability

The data used to support the findings of this study are included within the article.

Conflicts of Interest

The authors declare no conflict of interest.

Authors' Contributions

Song Xie was responsible for the writing—project administration. Ziyun Li was responsible for the original draft preparation project administration. Dongyan Liu and Qianghui Song were responsible for the resources. Peiyong Wang was responsible for the funding acquisition. Kaixi Xue was responsible for the data curation. All authors have read and agreed to the published version of the manuscript.

Acknowledgments

This research was funded by the Natural Science Foundation of Chongqing (Grant No. cstc2020jcyjmsxmX0558), the Open Fund of Chongqing Key Laboratory of Energy Engineering Mechanics & Disaster Prevention and Reduction (Grant No. EEMDPM2021206), the Logistics National Military Standard Project (No. BY120B009), and the Chongqing Postgraduate Education and Teaching Reform Research Project (No. yjg193145).

References

[1] J. Wang, J. Fu, W. Song, and Y. Zhang, "Mechanical properties, damage evolution, and constitutive model of rock- encased backfill under uniaxial compression," *Construction and Building Materials*, vol. 285, article 122898, 2021.

[2] H. Liu and L. Zhang, "A damage constitutive model for rock mass with nonpersistently closed joints under uniaxial compression," *Arabian Journal for Science and Engineering*, vol. 40, no. 11, pp. 3107–3117, 2015.

[3] H. Liu and T. Su, "A dynamic damage constitutive model for a rock mass with non-persistent joints under uniaxial compression," *Mechanics Research Communications*, vol. 77, pp. 12–20, 2016.

[4] B. Lin, P. Cao, S. Mao, C. Ou, and R. Cao, "Fatigue behaviour and constitutive model of yellow sandstone containing preexisting surface crack under uniaxial cyclic loading," *Theoretical and Applied Fracture Mechanics*, vol. 109, article 102776, 2020.

[5] X. S. Liu, J. G. Ning, Y. L. Tan, and Q. H. Gu, "Damage constitutive model based on energy dissipation for intact rock subjected to cyclic loading," *International Journal of Rock Mechanics and Mining Sciences*, vol. 85, pp. 27–32, 2016.

[6] Z. Zhou, Z. Li, C. Gao et al., "Peridynamic micro-elastoplastic constitutive model and its application in the failure analysis of rock masses," *Computers and Geotechnics*, vol. 132, article 104037, 2021.

[7] Z. Zhou, X. Li, Z. Ye, and K. Liu, "Obtaining constitutive relationship for rate-dependent rock in SHPB tests," *Rock Mechanics and Rock Engineering*, vol. 43, no. 6, pp. 697–706, 2010.

[8] Z. Han, D. Li, T. Zhou, J. Chen, and S. Xie, "Dynamic progressive fracture behavior of axially confined sandstone specimens containing a single flaw," *Theoretical and Applied Fracture Mechanics*, vol. 122, article 103597, 2022.

[9] D. Li, J. Jiang, and F. Gao, "Failure behavior of cuboid granite sample with a circular hole beneath a bonding fracture under biaxial compression," *Minerals*, vol. 12, no. 10, p. 1328, 2022.

[10] J. Feng, E. Wang, R. Shen, X. Li, and X. Xu, "Investigation on energy dissipation and its mechanism of coal under dynamic loads," *Geomechanics and Engineering*, vol. 11, no. 5, pp. 657–670, 2016.

[11] X. Kong, S. Li, E. Wang et al., "Dynamics behaviour of gas-bearing coal subjected to SHPB tests," *Composite Structures*, vol. 256, article 113088, 2021.

[12] X. Kong, E. Wang, X. He, E. Zhao, and C. Zhao, "Mechanical characteristics and dynamic damage evolution mechanism of coal samples in compressive loading experiments," *Engineering Fracture Mechanics*, vol. 210, pp. 160–169, 2019.

[13] X. Kong, E. Wang, S. Li, H. Lin, Z. Zhang, and Y. Ju, "Dynamic mechanical characteristics and fracture mechanism of gas-bearing coal based on SHPB experiments," *Theoretical and Applied Fracture Mechanics*, vol. 105, article 102395, 2020.

[14] L. Wang, H. Su, Y. Qin, and S. Chen, "Study on dynamic constitutive model of weakly consolidated soft rock in Western China," *Shock and Vibration*, vol. 2020, Article ID 8865013, 13 pages, 2020.

[15] Z. Wang, H. Shi, and J. Wang, "Mechanical behavior and damage constitutive model of granite under coupling of temperature and dynamic loading," *Rock Mechanics and Rock Engineering*, vol. 51, no. 10, pp. 3045–3059, 2018.

[16] J. Deng and D. Gu, "On a statistical damage constitutive model for rock materials," *Computers & Geosciences*, vol. 37, no. 2, pp. 122–128, 2011.

[17] Y. Zhai, F. Meng, Y. Li, Y. Li, R. Zhao, and Y. Zhang, "Research on dynamic compression failure characteristics and damage constitutive model of sandstone after freeze-thaw cycles," *Engineering Failure Analysis*, vol. 140, article 106577, 2022.

[18] G. Zhao, L. Xie, and X. Meng, "A damage-based constitutive model for rock under impacting load," *International Journal of Mining Science and Technology*, vol. 24, no. 4, pp. 505–511, 2014.

[19] Z. Li, S. Xie, Q. Song et al., "Energy dissipation and damage evolution characteristics of shale under triaxial cyclic loading and unloading," *Advances in Materials Science and Engineering*, vol. 2022, Article ID 1212584, 13 pages, 2022.

[20] W. Yao, T. He, and K. Xia, "Dynamic mechanical behaviors of Fangshan marble," *Journal of Rock Mechanics and Geotechnical Engineering*, vol. 9, no. 5, pp. 807–817, 2017.

[21] F. Wang, S. Liu, and L. Cao, "Research on dynamic compressive behaviors of marble under high strain rates with split Hopkinson pressure bar," *Advances in Materials Science and Engineering*, vol. 138, Article ID 104095, 2020.

[22] D. Ai, Y. Zhao, Q. Wang, and C. H. Li, "Experimental and numerical investigation of crack propagation and dynamic properties of rock in SHPB indirect tension test," *International Journal of Impact Engineering*, vol. 126, pp. 135–146, 2019.

[23] X. Li, Z. Zhou, T.-S. Lok, L. Hong, and T. Yin, "Innovative testing technique of rock subjected to coupled static and dynamic loads," *International Journal of Rock Mechanics and Mining Sciences*, vol. 45, no. 5, pp. 739–748, 2008.

[24] H. Gu, M. Tao, X. Li, W. Gao, and Q. Li, "Dynamic tests and mechanical model for water-saturated soft coal with various particle gradations," *International Journal of Rock Mechanics and Mining Sciences*, vol. 132, article 104386, 2020.

[25] N. Wu, J. Fu, Z. Zhu, and B. Su, "Experimental study on the dynamic behavior of the Brazilian disc sample of rock material," *International Journal of Rock Mechanics and Mining Sciences*, vol. 130, article 104326, 2020.

[26] M. Tao, H. Zhao, X. Li, J. Ma, K. Du, and X. Xie, "Determination of spalling strength of rock by incident waveform," *Geomechanics & engineering*, vol. 12, no. 1, pp. 1–8, 2017.

[27] D. Li, Z. Han, X. Su, T. Zhou, and X. Li, "Dynamic mechanical properties and fracturing behavior of marble specimens containing single and double flaws in SHPB tests," *Rock Mechanics and Rock Engineering*, vol. 52, no. 6, pp. 1623–1643, 2019.

[28] R. Shan, Y. Jiang, and B. Li, "Obtaining dynamic complete stress–strain curves for rock using the split Hopkinson pressure bar technique," *International Journal of Rock Mechanics and Mining Sciences*, vol. 37, no. 6, pp. 983–992, 2000.

[29] J. Zhang, S. Guo, X. Zhang, L. Wang, Y. Cao, and G. Liu, "Dynamic damage constitutive model of plastic hardening-softening process of coal under impacting loading," *Journal of China Coal Society*, vol. 46, pp. 759–769, 2021.

[30] Q. Ma, Y. Tan, X. Liu, Q. Gu, and X. Li, "Effect of coal thicknesses on energy evolution characteristics of roof rock-coal-floor rock sandwich composite structure and its damage constitutive model," *Composites Part B: Engineering*, vol. 198, article 108086, 2020.

[31] V. Hucka and B. Das, "Brittleness determination of rocks by different methods," *International Journal of Rock Mechanics and Mining Sciences & Geomechanics Abstracts*, vol. 11, no. 10, pp. 389–392, 1974.

[32] L. Qiao, J. Hao, Z. Liu, Q. Li, and N. Deng, "Influence of temperature on the transformation and self-control of energy during sandstone damage: experimental and theoretical research," *International Journal of Mining Science and Technology*, vol. 32, no. 4, pp. 761–777, 2022.

[33] G. Wang, R. Wang, F. Sum et al., "Analysis of nonlinear energy evolution in fractured limestone under uniaxial compression," *Theoretical and Applied Fracture Mechanics*, vol. 120, article 103387, 2022.

[34] F. Meng, H. Zhou, C. Zhang, R. Xu, and J. Lu, "Evaluation methodology of brittleness of rock based on post-peak stress–strain curves," *Rock Mechanics and Rock Engineering*, vol. 48, no. 5, pp. 1787–1805, 2015.

[35] F. Meng, L. N. Y. Wong, and H. Zhou, "Rock brittleness indices and their applications to different fields of rock engineering: a review," *Journal of rock mechanics and geotechnical Engineering*, vol. 13, no. 1, pp. 221–247, 2021.